Appendix A. Temporal sequence of stream temperature records from the Boise River basin used to parameterize temperature models (n = 780).

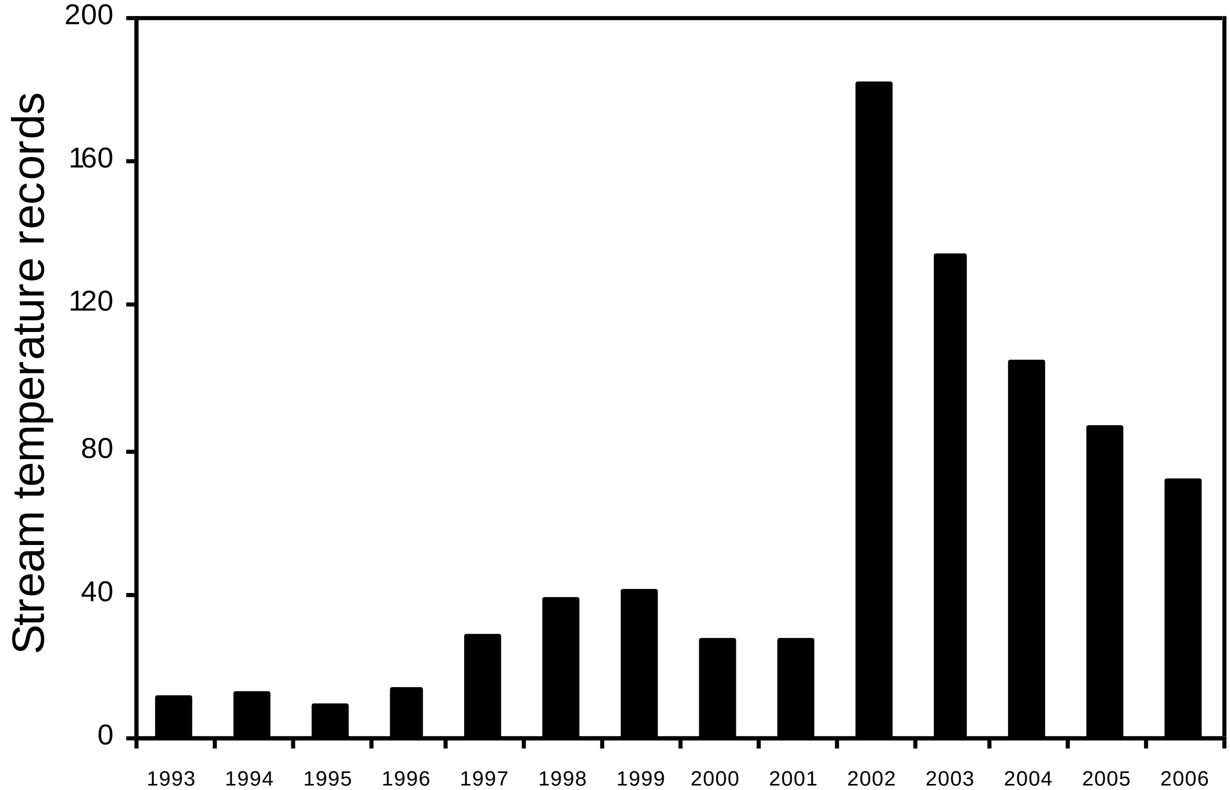

Appendix B. Changes in riparian vegetation determined from Thematic Mapper satellite imagery relative to wildfire perimeters within the Boise River basin between 1989 and 2002.

	TM Classification					
Fire Perimeter	1989	2002	Cell count	Cell changes	Cells with vegetation loss	Cells with vegetation gain
Inside	Open	Open	130636			
	Open	Shrub	9602	9602		9602 (60.2%)
	Open	Tree	4227	4227		4227 (26.5%)
	Shrub	Open	8173	8173	8173 (8.10%)	
	Shrub	Shrub	17628			
	Shrub	Tree	2116	2116		2116 (13.3%)
	Tree	Open	71483	71483	71483 (70.6%)	
	Tree	Shrub	21558	21558	21558 (21.3%)	
	Tree	Tree	43417			
	Water	Water	2125			
		Total =	310965	117159 (37.7%)	101214 (32.6%)	15945 (5.13%)
Outside	Open	Open	278725			
	Open	Shrub	46585	46585		46585 (37.0%)
	Open	Tree	55188	55188		55188 (43.8%)
	Shrub	Open	14708	14708	14708 (13.0%)	
	Shrub	Shrub	102933			
	Shrub	Tree	24300	24300		24300 (19.3%)
	Tree	Open	42203	42203	42203 (37.3%)	
	Tree	Shrub	56176	56176	56176 (49.7%)	
	Tree	Tree	363934			
	Water	Water	20742			
		Total =	1005494	239160 (23.8%)	113087 (11.3%)	126073 (12.5%)

Appendix C. An example of riparian vegetation classifications derived from Thematic Mapper satellite imagery before a wildfire in 1989 (a) and after fire in 2002 (b). Classifications mapped as vegetative gains and losses (c).

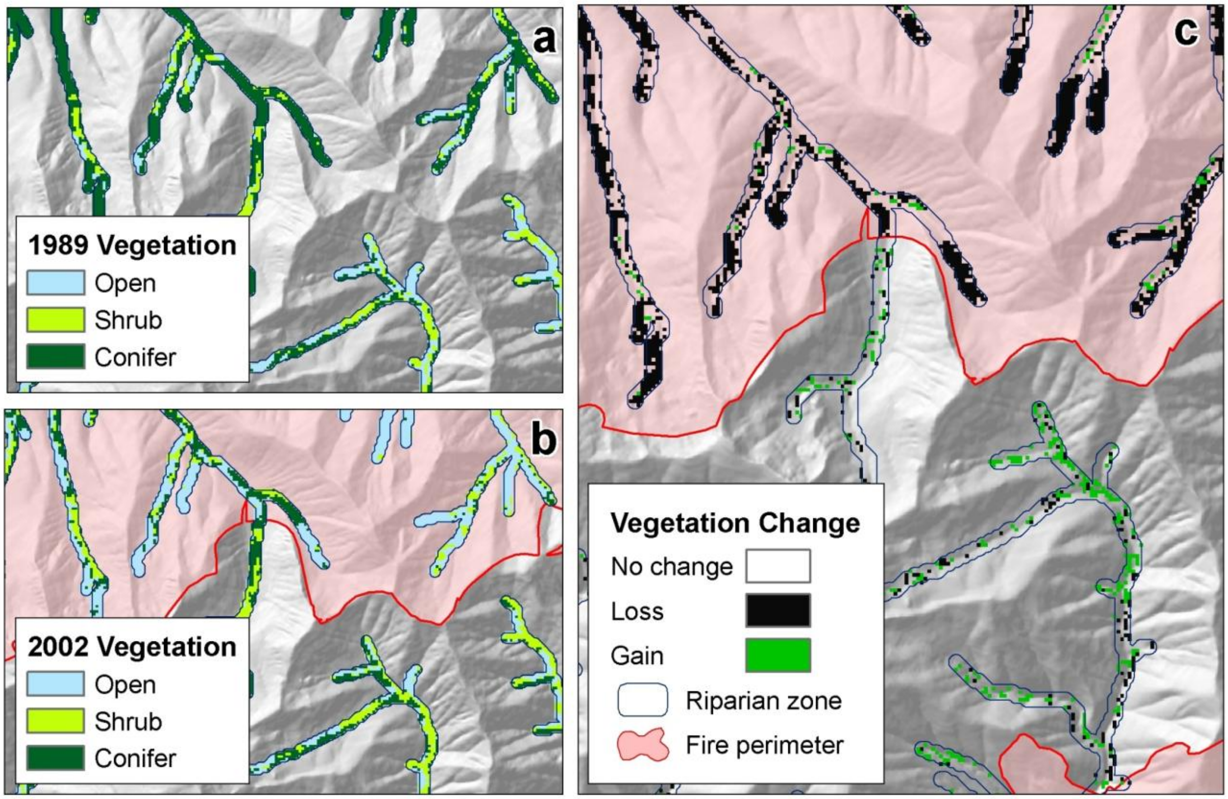

Appendix D. Relationships between radiation, watershed area, and vegetation class used to predict radiation values for the stream network in the BRB. Vegetation classifications were derived from Thematic Mapper imagery and radiation was measured at 181 field sites using hemispherical photography. Because the vegetation classification did not account for variation in vegetative height, density, or species composition within or among individual pixels, considerable variation occurred in the power-law relationships we developed. Despite these omissions, however, the approach did capture predictable distinctions between vegetation types and proved adequate for describing dramatic changes in vegetative structure and radiation inputs that occurred after fires (Appendix C).

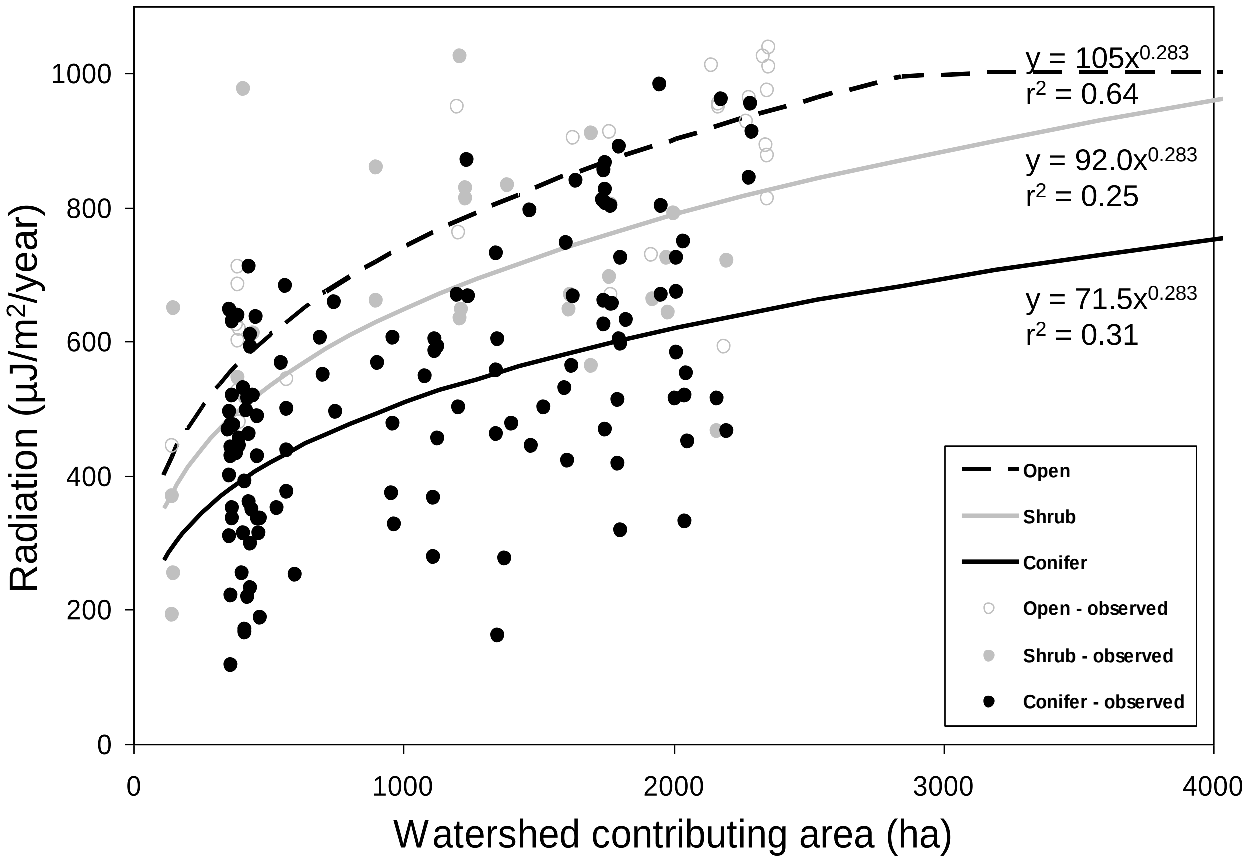

Appendix E. Stream temperature thresholds used to delineate habitat quality for bull trout (left panels) and rainbow trout (right panels). Thresholds were based on observed densities of bull trout < 150 mm and rainbow trout collected during electrofishing surveys of 249 sites on 20 streams in or near the Boise River basin in 2007. Temperatures in several of the warmest sites where bull trout occurred were affected by fires after surveys were complete. Rainbow trout probably occurred in streams warmer than those we sampled, as Dunham et al. (2007) observed rainbow trout in Boise River basin sites with MWMTs exceeding 25.5°C and there are several published accounts of rainbow trout in streams as warm as 27°C - 28°C (McCullough et al. 2001).

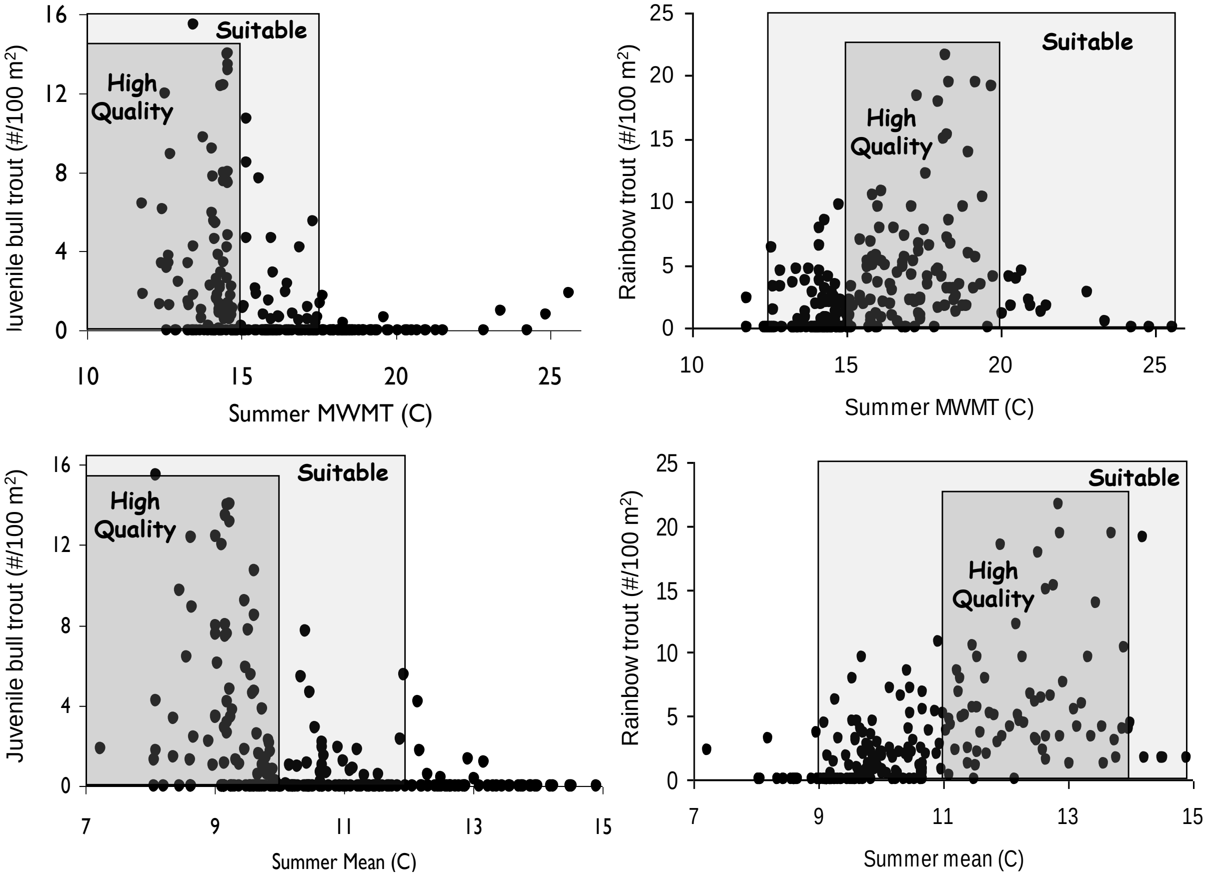

Appendix F. Correlations among variables at 780 sites used in stream temperature models for the Boise River basin.

	C_A	D_D	Ele	G_V	SL	V_B	Rad	Air MWMT	Air mean	Flow	Stream mean	Stream MWMT
C_A	1.00											
D_D	0.14	1.00										
Ele	-0.32	-0.54	1.00									
G_V	-0.08	-0.23	0.52	1.00								
SL	-0.15	-0.30	0.26	0.13	1.00							
V_B	0.24	0.09	0.00	0.24	-0.44	1.00						
Rad	0.33	0.11	-0.30	0.01	-0.40	0.34	1.00					
Air MWMT	-0.02	0.01	0.00	-0.09	-0.08	-0.09	-0.13	1.00				
Air mean	0.02	0.11	-0.12	-0.09	-0.11	0.02	0.09	0.66	1.00			
Flow	-0.05	-0.01	0.02	0.21	0.09	0.02	0.18	-0.63	0.02	1.00		
Stream mean	0.41	0.33	-0.72	-0.45	-0.25	0.11	0.46	0.12	0.25	-0.16	1.00	
Stream MWMT	0.29	0.30	-0.60	-0.39	-0.29	0.17	0.46	0.14	0.19	-0.18	0.93	1.00

Appendix G. Semivariograms of the residuals from the final MWMT (left panels) and summer mean (right panels) spatial stream temperature models, which included autocovariance structures based on flow-connected, flow-unconnected, and Euclidean relationships. Semivariograms quantify the average variability between pairwise combinations of model residuals for a series of spatial lags and plot this variability as a function of the intervening distance. Semivariograms of the temperature models suggested strong spatial trends in residuals based on Euclidean and flow-connected distances; with weaker trends among flow-unconnected sites.

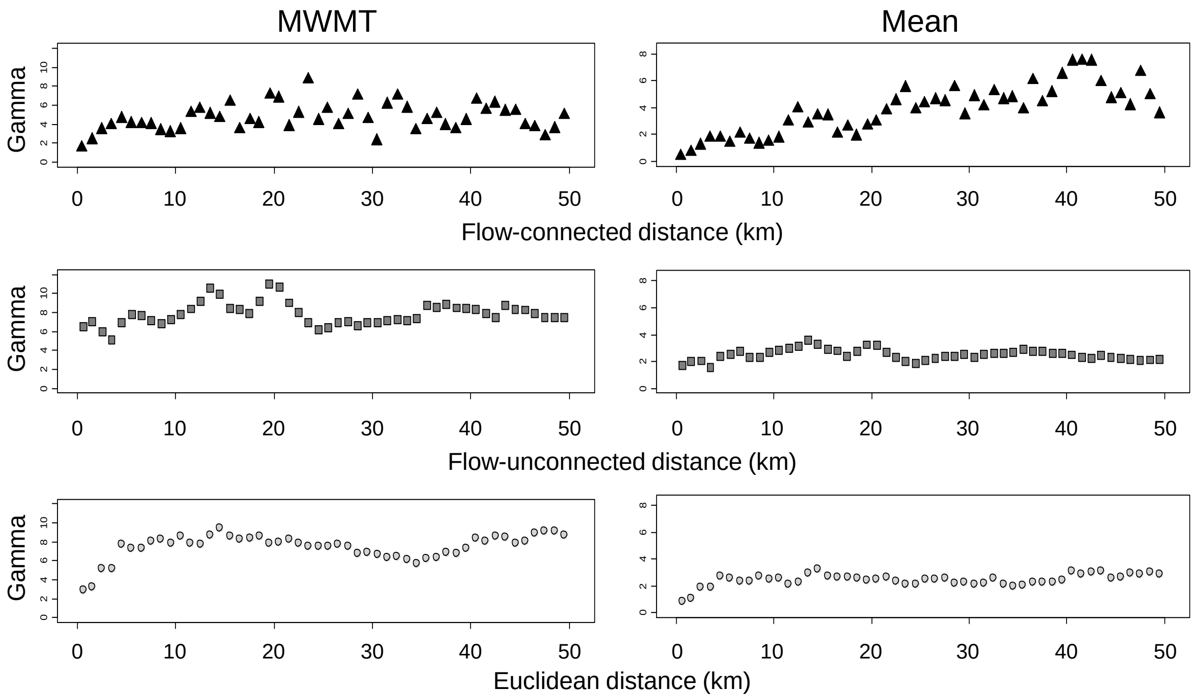

Appendix H. Percentage of the residual error structures in the final spatial stream temperature models attributable to tail-up, tail-down, Euclidean, and nugget portions of the covariance structure. The tail-up portion of the covariance structure explained the greatest residual variation, which is generally expected for stream attributes with passive flow characteristics.